Biophysical Journal, Volume 99

Supporting Material

Molecular Simulation of the Effect of Cholesterol on Lipid-Mediated Protein-Protein Interactions

Frédérick J.-M. de Meyer, Jocelyn M. Rodgers, Thomas F. Willems, and Berend Smit

Molecular simulation of the effect of cholesterol on lipid-mediated protein-protein interactions: Supplementary Information.

Frédérick J.-M. de Meyer [1]
Dept. of Chemical and Biomolecular Engineering, University of California, Berkeley, CA 94720, USA
Materials Science Division, Lawrence Berkeley National Laboratory, Berkeley, CA 94720, USA

Jocelyn M. Rodgers
Physical Biosciences Division, Lawrence Berkeley National Laboratory, Berkeley, CA 94720, USA

Thomas F. Willems
Dept. of Chemical and Biomolecular Engineering, University of California, Berkeley, CA 94720, USA

Berend Smit
Dept. of Chemical and Biomolecular Engineering, University of California, Berkeley, CA 94720, USA
Dept. of Chemistry, University of California, Berkeley, CA 94720, USA
Materials Science Division, Lawrence Berkeley National Laboratory, Berkeley, CA 94720, USA

[1]Dept. of Chemical Engineering, University of California, Berkeley, 101B Gilman Hall #1462, Berkeley CA 94720-1462, USA. Tel.: +1 (510) 642 9275/7260, Fax: +1 (510) 642 8063

1 MC-DPD Simulations

The mesoscopic model was studied with the DPD simulation technique (1–3). In DPD, pairwise additive and momentum conserving dissipative and random forces are added to the pairwise additive conservative force in order to reintroduce the correct hydrodynamic behavior. Newton's laws were assumed to be applicable and the resulting equations of motion were integrated using a modified version of the velocity Verlet algorithm (3), with the timestep 0.03. For a detailed description of the simulation method, and its applications, we refer to previous articles (4–6).

In our model, the conservative force comprises two contributions. The first contribution represents non-bonded interactions and is chosen in such a way as to model the direct, effective interactions between every two beads within a cut-off diameter $R_{\rm c}$ of 6.46 Å by a soft-repulsive potential:

$$\mathbf{F}_{ij}^{C} = \begin{cases} a_{ij}(1 - r_{ij}/R_{\rm c})\hat{\mathbf{r}}_{ij} & (r_{ij} < R_{\rm c}) \\ 0 & (r_{ij} \geq R_c) \end{cases} \tag{1}$$

The second contribution takes into account bonded interactions and contains an elastic contribution

$$\mathbf{F}_{\rm spring} = -K_r(r_{ij} - r_{\rm eq})\hat{\mathbf{r}}_{ij}, \tag{2}$$

which describes the harmonic force used to tie two consecutive beads in the chain of either a lipid or a cholesterol, and a bond-bending force

$$\mathbf{F}_{\theta} = -\nabla\left(\frac{1}{2}K_{\theta}(\theta - \theta_o)^2\right), \tag{3}$$

between consecutive bonds, to control the chain flexibility.

Only the conservative part of the force determines the equilibrium averages of the system observables. In this way, DPD can be seen as a momentum-conserving thermostat for MD simulations.

Within the DPD approach, reduced units are usually adopted. The unit of length is the cutoff radius R_c. The number of atoms or molecules represented by a DPD bead is the renormalization factor for expressing the cutoff radius R_c in physical units. By representing three water molecules as one coarse grained bead and considering that a water molecule has approximately a volume of 30 Å^2, one obtains R_c= 6.46 Å for a bead density $\rho = 3$.

The numerical values of the repulsion parameters (see 1) for the interaction between bead types are the same used by Venturoli *et al.* (5), and are reported in Figure 1 in the main text. The parameters for the elastic contribution to the interaction energy (2) have the values $r_{\rm eq}$=0.7 and K_r=100 for all bonds and the parameters for the bond-bending force (3) are K_θ=6 and $\theta_o = 180°$ for the bonds between consecutive lipid and cholesterol tail beads, K_θ=3 and $\theta_o = 90°$ for the bonds between the head-bead connected to the lipid tails and the first bead in both tails (7) and K_θ=100 and $\theta_o = 60°$ or $\theta_o = 150°$ for the stiff cholesterol ring. The units of K_r and K_θ are E_0/R_C^2 and E_0/rad^2, respectively, where E_0 is the reduced energy unit.

Because unconstrained lipid bilayers are essentially in a tensionless state (8), we reproduced this condition by simulating the system in the $NP_\perp\gamma T$ ensemble, where γ is the surface tension of the lipid bilayer. Previous simulation studies were done in the $NV\gamma T$ (9). However, simulations in both ensembles gave very similar results. We simulate in the $NP_\perp\gamma T$ ensemble via a hybrid Monte Carlo (MC) and dissipative particle dynamics (DPD) approach. Each cycle of the simulation consists of one of the following possible moves: (1) a DPD trajectory of 1 to 50 steps which applies a thermostat to the dynamics, (2) a constant surface tension MC move, and (3) a constant normal pressure MC move. These moves are chosen with a likelihood of 60% - 20% - 20%.

The Monte Carlo moves are carried out in order to allow relevant degrees of freedom to relax during simulations as temperature varies. These relevant degrees of freedom include the density of the box and the surface area of the lipid bilayer. As such, in the following discussions, the particle positions are described via the collective coordinates s^N where any position r may be obtained via $r = (L_x s_x, L_y s_y, L_z s_z)$ and the x-direction is chosen to be perpendicular to the lipid bilayer surface.

Surface area is allowed to vary via the constant surface tension MC move because lipid bilayer areas are known to vary with the temperature and the phase of the bilayer. As described in previous papers (10), the constant surface tension MC move alters the lateral surface area of the lipid bilayer while maintaining a constant volume in order to do no work against external pressure. The moves are executed in order to sample from the following partition function, expressing particle positions in terms of reduced positions s:

$$Z_{NV\gamma T} = \frac{V^N}{\Lambda^{3N} N!} \frac{1}{L_0} \int_0^\infty dL_y \int dL_z \delta(L_y - L_z) e^{\beta\gamma L_y L_z} \times \int dL_x \delta\left(L_x - \frac{V}{L_y L_z}\right) \int ds^N \exp\left(-\beta U(s^N; L_y)\right). \quad (4)$$

A random step in the box length L_y is chosen and L_z is changed identically while L_x is changed in order to maintain a constant volume. The surface tension γ is set to zero.

We now also maintain a constant pressure applied normal to the lipid bilayer via an additional MC move. Application of the constant normal pressure allows for varying degrees of lipid head group hydration from the water molecules while maintaining a well-defined bulk water reservoir. In reduced units, $P_\perp = 22.28$, the pressure of bulk water at $\rho = 3.0$ and $T = 0.32$. This temperature was chosen because it corresponds to the temperature at which the water compressibility is matched for $a_{ww} = 25$, when grouping three water molecules per bead, according to work by Groot and Warren (3). Constant pressure moves were chosen to sample from the partition function:

$$Z_{NP_\perp AT} = \frac{1}{\Lambda^{3N} N!} \frac{1}{V_0} \int_0^\infty dV V^N e^{-\beta p V} \int dL_x \delta\left(L_x - \frac{V}{A}\right) \times \int ds^N \exp\left(-\beta U(s^N; L_x)\right). \quad (5)$$

A random step in the box volume V is chosen and then solely the simulation box length L_x is varied. This approach ensures that no work is done relative to the surface tension during

the constant pressure simulation moves. For a transformation from V_o to V_n, the acceptance probability is defined as

$$(V_o \rightarrow V_n) = \min \left[1, \left(\frac{V_n}{V_o} \right)^N \exp \left(-\beta p \Delta V - \beta \Delta U \right) \right]. \quad (6)$$

In this acceptance probability, the volume ratio is raised to the total number of molecules (not individual beads) because during the constant pressure moves all relative intramolecular coordinates are held constant.

2 Previous Applications of the Model

Previously, Kranenburg *et al.* and Venturoli *et al.* developed a mesoscopic model of a hydrated lipid bilayer and transmembrane proteins, respectively (4, 5, 11). The phase behavior of the saturated lipid model and the adaptation of the bilayer and the protein to hydrophobic mismatch agree very well with the experimental observations (11). We used this mesoscopic model to study the potential of mean force (PMF) between two proteins as a function of hydrophobic mismatch and protein diameter (6). We extended this model of a hydrated phospholipid bilayer to include cholesterol (9, 12). This model correctly describes the effects of cholesterol on the mechanical and structural properties of a saturated phosphatidylcholine bilayer and reproduces the main features of the experimental cholesterol-saturated phospholipid phase diagram (9, 12). In this paper, we combine the mesoscopic models of water, lipid, cholesterol, and protein to study the effect of cholesterol on the protein-protein interactions.

3 Potential of Mean Force

The potential of mean force (PMF) as a function of the distance ξ between the centers of mass of two proteins (or cluster of proteins) quantifies the effective interaction between two proteins. The PMFs were computed using a similar method as described in detail in (6). A first estimation of the PMF was obtained using umbrella sampling with a harmonic heavyside biased potential. To unbias we used the weighted histogram analysis method (WHAM) (13, 14). We performed a forward and a backward PMF calculation. In a second step the biased potential is the sum of a heavyside potential and the inverse average PMF obtained from the previous step. This step was repeated, updating the PMF, until all the individual histograms of the windows showed a uniform distribution. Generally, 3 to 10 iterations were required to satisfy this condition.

4 Hydrophilic Shielding Parameter

To characterize the extent in which the bilayer screens the hydrophobic parts of the lipids and the peptides, we introduced the concept of hydrophilic shielding (6). Within this concept, the protein interactions are interpreted as resulting from the dynamic reorganization of the entire system to maintain an optimal hydrophilic shielding of the protein and lipid hydrophobic

parts, constrained by the flexibility of the components. For this we define the lipid head fraction as the number of lipid head beads at a given position in the plane of the lipid bilayer in which the protein is embedded divided by the average number of lipid head beads of a pure bilayer without embedded proteins. The lipid tail fraction is defined in an analogous way. The hydrophilic shielding parameter, defined at every position in the plane of a lipid bilayer, is the ratio of the lipid head fraction and the lipid tail fraction, and is a measure for the relative number of hydrophilic beads shielding the hydrophobic tail beads from the water at a given position. This parameter is one at sufficient distances from a protein. When the hydrophilic shielding parameter is bigger than one, the density of the lipid heads shielding the lipid tails present is higher than in the pure lipid bilayer.

5 Hydrophobic Thickness Profile

In the Figure below, the hydrophobic thickness of the bilayer around the two large proteins with positive mismatch is shown. One can see that the hydrophobic thickness of the bilayer increases by only 1.2 Å due to the addition of cholesterol. The different hydrophobic thickness profiles in between both proteins reflect the different ways bilayers with and without cholesterol adapt to the approach of both molecules. It seems that in a lipid bilayer without cholesterol it is difficult to maintain the negative curvature in between both proteins when they are close. When cholesterol, which has an intrinsic negative curvature, is added to the bilayer, the region between the two approaching proteins has a nice negative curvature until both proteins touch.

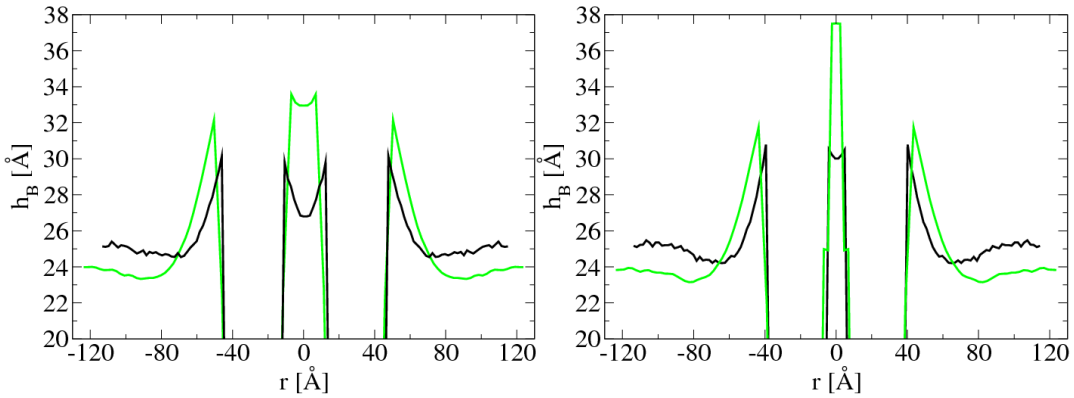

Figure 1: Hydrophobic thickness around two large proteins. Simulations were performed in a $h_3(t_5)_2$ bilayer without (green lines) and with (black lines) 40 mol% cholesterol. The proteins are at a distance of 58 Å (a) and 45 Å (b). Proteins have a diameter of 32 Å and a positive mismatch of +7 Å. ΔT=0.28.

6 Cholesterol Distribution Around a Protein

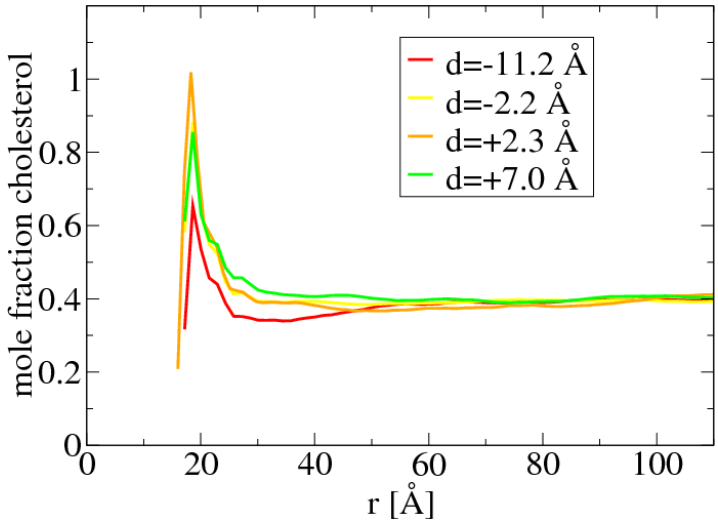

Figure 2: Mole fraction of cholesterol, as function of the distance r from the center of mass of a large protein with diameter 32 Å with a negative mismatch of -11.2 Å, negligible mismatch of -2.2 Å and positive mismatch of +2.3 and +7 Å, in a $h_3(t_5)_2$ bilayer with 40 mol% cholesterol. ΔT=0.28.

7 Snapshots Protein Clustering

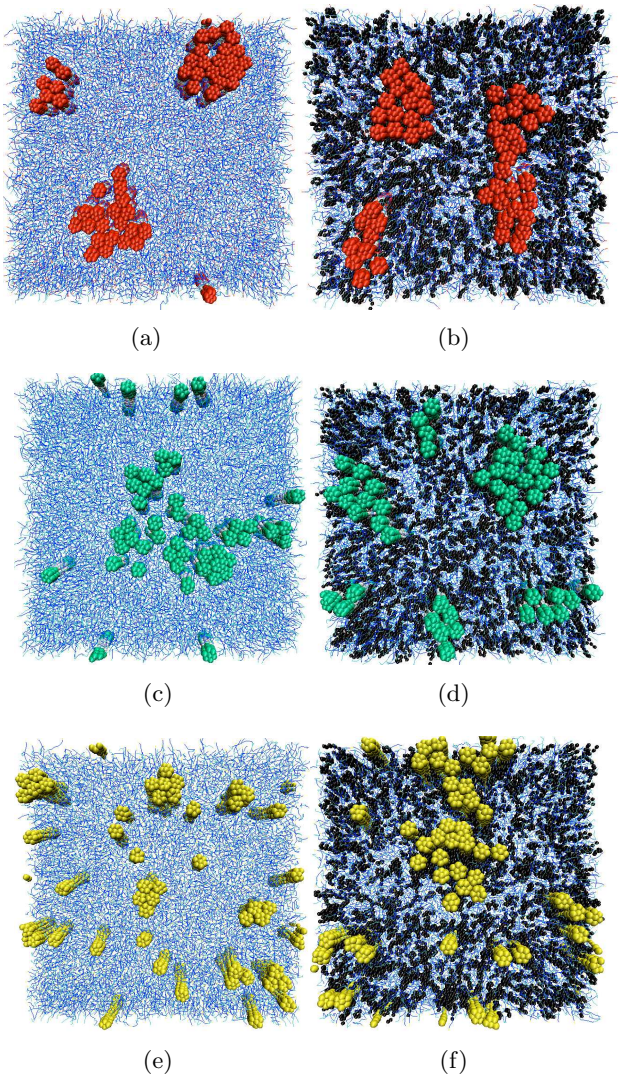

Figure 3: Snapshot of a top view of a lipid bilayer after 10^6 MC-DPD cycles. The lipids are depicted in blue, cholesterol in black. Proteins with a negative mismatch of -10 Å are red (a,b), with a negative mismatch of -5.5 Å are dark green (c,d) and with a negligible mismatch of -1 Å are yellow (e,f). Water beads are not shown for clarity. Periodic boundary conditions apply. Initially the proteins were mixed and embedded as far as possible from each other. In (b,d,f), the $h_3(t_5)_2$ bilayer contains 40 mol% cholesterol. ΔT=0.28. The addition of cholesterol changes the mismatch by -1.2 Å.

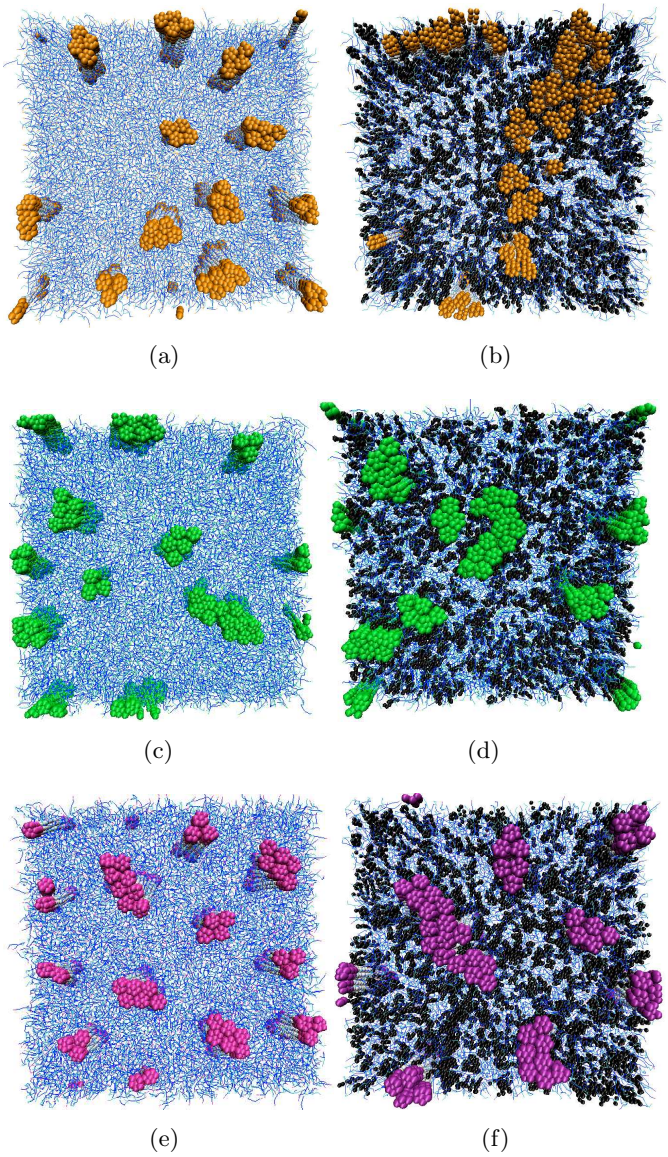

Figure 4: Snapshot of a top view of a lipid bilayer after 10^6 MC-DPD cycles. The lipids are depicted in blue, cholesterol in black. Proteins with a positive mismatch of +3.5 Å are orange (a,b), with a positive mismatch of +8.1 Å are green (c,d) and with a positive mismatch of +16.3 Å are pink (e,f). In (b,d,f), the $h_3(t_5)_2$ bilayer contains 40 mol% cholesterol. ΔT=0.28. The addition of cholesterol changes the mismatch by -1.2 Å.

8 PMFs Protein Clustering

We computed the potential of mean force between two proteins, in bilayers with and without cholesterol. Using geometric arguments one can see that a cluster of 7 proteins is relatively stable under mismatch conditions. To obtain some insights in the clustering behavior, we also computed the PMFs between a cluster of 7 proteins and a single protein and between two clusters of 7 proteins:

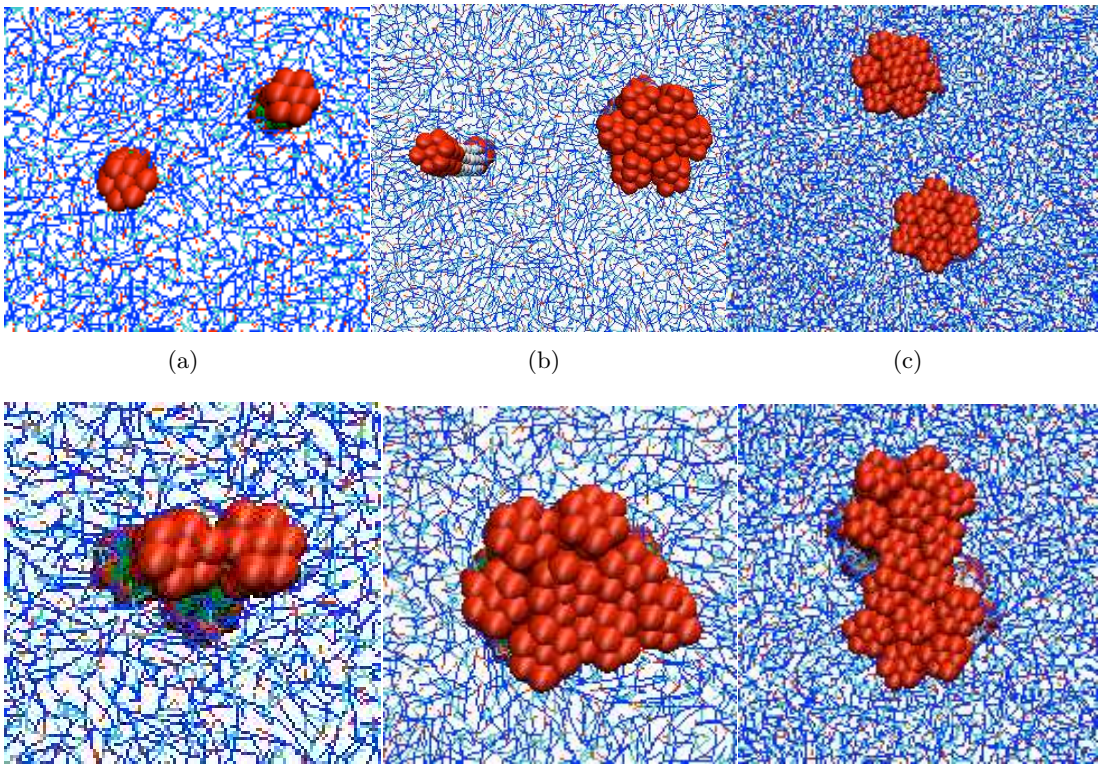

Figure 5: Protein and protein cluster configurations related to the PMF calculations. Snapshot of a a top view of a lipid bilayer. The lipids are depicted in blue, the proteins in red. (a), (b) and (c) correspond with the dissociated configuration for the 1-1, 7-1 and 7-7 PMF calculations, respectively. (d), (e) and (f) illustrate the associated configurations for the 1-1, 7-1 and 7-7 PMF calculations, respectively. In the associated configuration both clusters are in close contact, as shown in the pictures. The further merging of clusters is not described.

Negative Mismatch The four PMFs have a very similar nature. The minimum value of the free energy for the 14-mer is lower than for the dimer and the well is always slightly deeper in the bilayer with cholesterol.

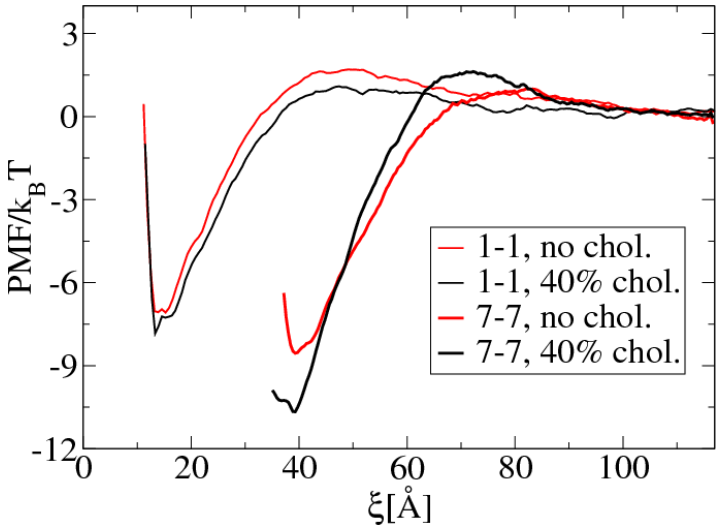

Figure 6: Potential of mean force as a function of the distance ξ between two proteins (1-1) and between two clusters of 7 protein (7-7) in a $h_3(t_5)_2$ bilayer without (red) and with (black) 40 mol% cholesterol. ΔT=0.28. The proteins have a negative mismatch of -10 Å in the pure bilayer and -11.2 Å when cholesterol is added.

Positive Mismatch For proteins with positive mismatch, we observe that cholesterol dramatically decreases aggregation barriers.

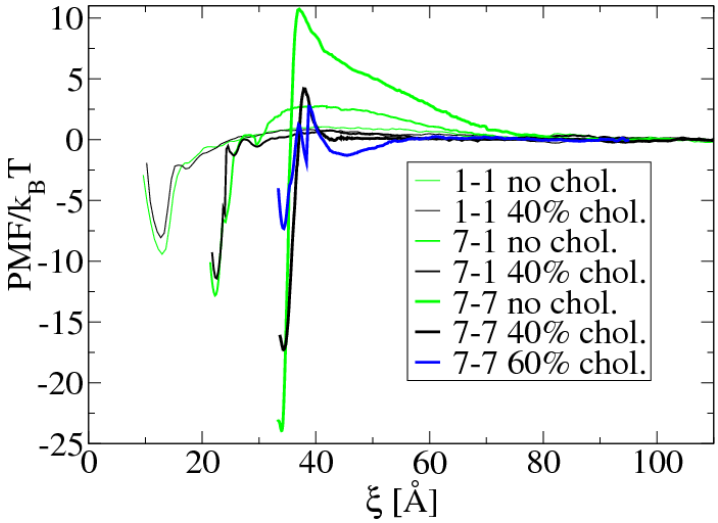

Figure 7: Potential of mean force as a function of the distance ξ between two proteins (1-1), between a single protein and a cluster of seven proteins (1-7) and between two clusters of 7 proteins (7-7) in a $h_3(t_5)_2$ bilayer without green), with 40 mol% (black) and with 60 mol% (blue) cholesterol. ΔT=0.28. The proteins have a positive mismatch of +8.1 Å in the pure bilayer and +7 Å when cholesterol is added.

9 Selectivity

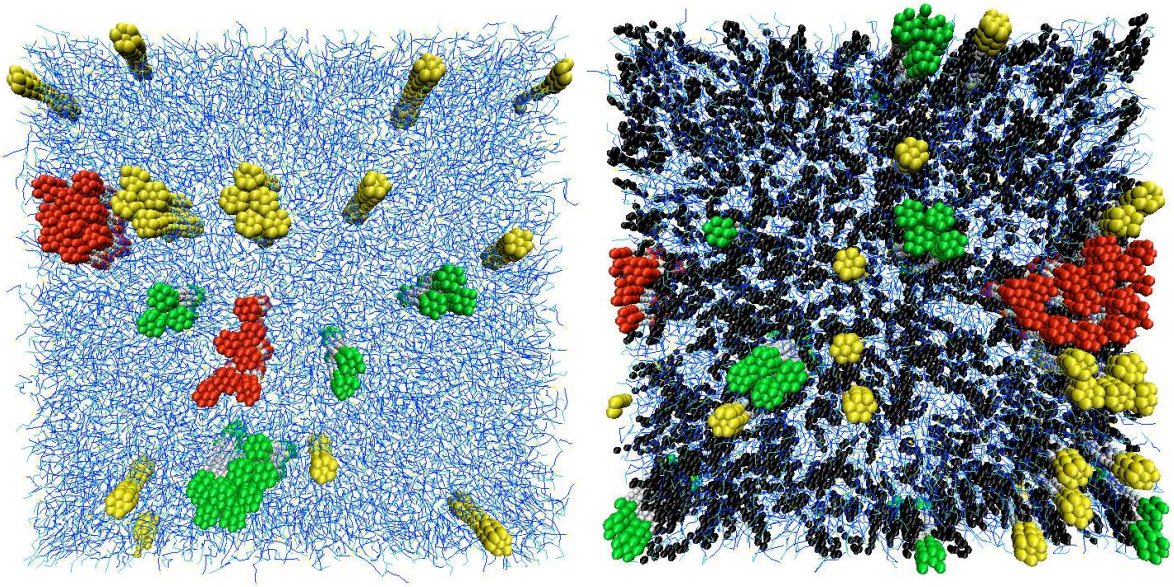

(a) (b)

Figure 8: Snapshot of a top view of a lipid bilayer after 10^6 MC-DPD cycles. The bilayer in (a) and (b) contains 3 different types of proteins. The $h_3(t_5)_2$ lipids are depicted in blue, cholesterol in black. Proteins with a negative mismatch of -10 Å are red, with negligible mismatch of -1 Å are yellow and with a positive mismatch of +8.1 Å are green. Water beads are not shown for clarity. Periodic boundary conditions apply. Initially the proteins were mixed and embedded as far as possible from each other. In (b), the bilayer contains 40 mol% cholesterol. The addition of cholesterol changes the mismatch by -1.2 Å. ΔT=0.28.

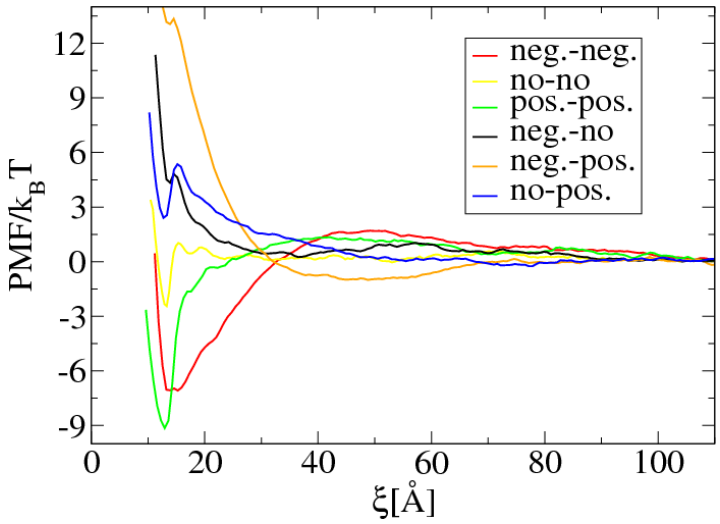

(a)

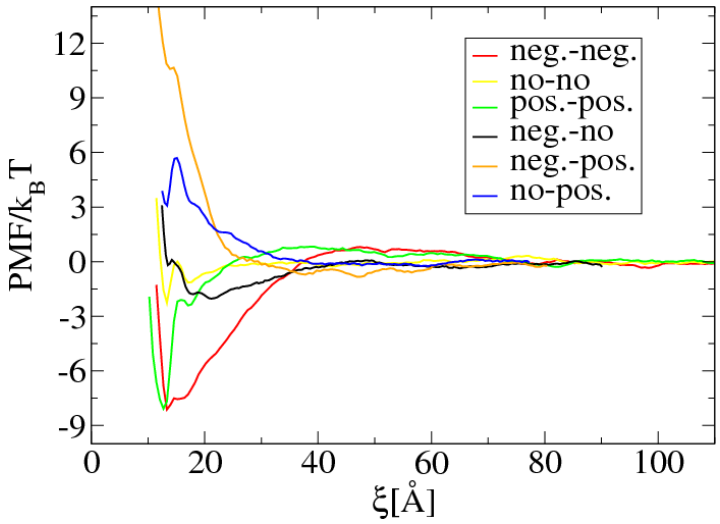

(b)

Figure 9: Potential of mean force as a function of the distance ξ between two proteins (1-1) in a $h_3(t_5)_2$ bilayer without (a) and with (b) 40 mol% cholesterol. The six PMFs describe the six possible single protein - single protein interactions that might occur in the system shown above. Negative mismatch is -10 Å, negligible mismatch is -1 Å and positive mismatch is +8.1 Å. The addition of cholesterol changes the mismatch by -1.2 Å. ΔT=0.28.

10 Error bars PMF

At long distances between the proteins, the PMF should be zero. Fluctuations of the PMF around zero at long distances give a good idea of the error. When we calculated the PMFs we noticed that between subsequent iterations, the values of the free energy minima and maxima, when the proteins are at close distance, were most prone to fluctuations. In the Figure below we show the error on the PMF calculation for a specific example.

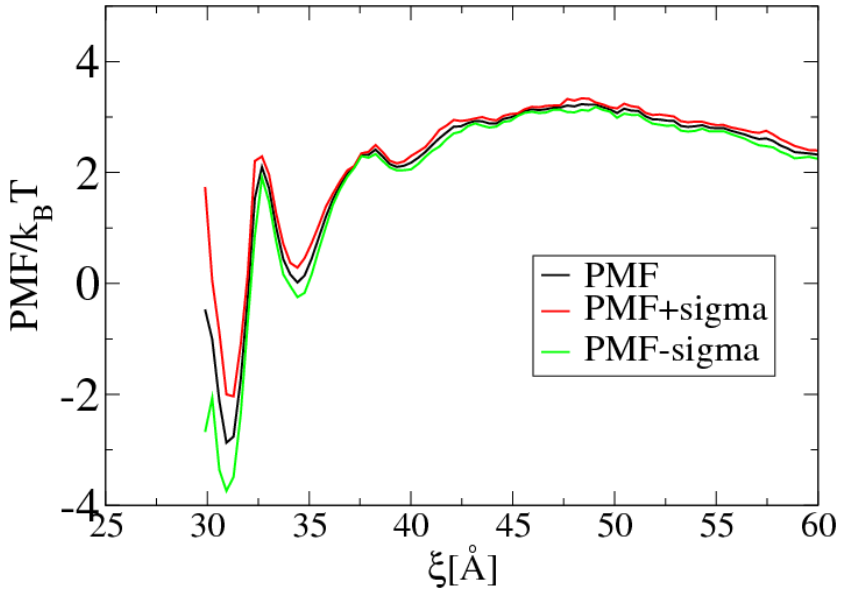

Figure 10: Potential of mean force with errors as a function of the distance ξ between two proteins (diameter 32 Å) in a $h_3(t_5)_2$ bilayer. The positive mismatch is 8 Å. ΔT=0.28. Sigma is the standard deviation.

References

1. Hoogerbrugge, P. J., and J. M. V. A. Koelman, 1992. Simulating microscopic hydrodynamics phenomena with dissipative particle dynamics. *Europhys. Lett.* 19:155–160.

2. Español, P., and P. B. Warren, 1995. Statistical mechanics of dissipative particle dynamics. *Europhys. Lett.* 30:191–196.

3. Groot, R. D., and P. B. Warren, 1997. Dissipative particle dynamics: bridging the gap between atomistic and mesoscopic simulation. *J. Chem. Phys.* 107:4423–4435.

4. Kranenburg, M., and B. Smit, 2005. Phase behavior of model lipid bilayers. *J. Phys. Chem. B* 109:6553–6563.

5. Venturoli, M., B. Smit, and M. M. Sperotto, 2005. Simulation studies of protein-induced

bilayer deformations, and lipid-induced protein tilting, on a mesoscopic model for lipid bilayers with embedded proteins. *Biophys. J.* 88:1778–1798.

6. de Meyer, F. J.-M., M. Venturoli, and B. Smit, 2008. Molecular simulations of lipid-mediated protein-protein interactions. *Biophys. J.* 95:1851–1865.

7. Kranenburg, M., J.-P. Nicolas, and B. Smit, 2004. Comparison of mesoscopic phospholipid-water models. *Phys. Chem. Chem. Phys.* 6:4142 – 4151.

8. Marrink, S. J., E. Lindahl, O. Edholm, and A. E. Mark, 2001. Simulation of the spontaneous aggregation of phospholipids into bilayers. *J. Am. Chem. Soc.* 123:8638–8639.

9. de Meyer, F. J.-M., and B. Smit, 2009. Effect of cholesterol on the structure of a phospholipid bilayer. *Proc. Natl. Acad. Sci. USA* 106:3654–3658.

10. Kranenburg, M., M. Venturoli, and B. Smit, 2003. Phase behavior and induced interdigitation in bilayers studied with dissipative particle dynamics. *J. Phys. Chem. B* 107:11491–11501.

11. Venturoli, M., M. M. Sperotto, M. Kranenburg, and B. Smit, 2006. Mesoscopic models of biological membranes. *Phys. Rep.* 437:1–57.

12. de Meyer, F. J.-M., A. Benjamini, J. Rodgers, Y. Misteli, and B. Smit, 2010. Molecular simulation of the DMPC-cholesterol phase diagram. *J. Phys. Chem. B* 114:10451–10461.

13. Kumar, S., D. Bouzida, R. H. Swendsen, P. A. Kollman, and J. M. Rosenberg, 1992. The weighted histogram analysis method for free-energy calculations on biomolecules. I. The method. *J. Comp. Chem.* 13:1011–1021.

14. Souaille, M., and B. Roux, 2001. Extension to the weighted histogram analysis method: combining umbrella sampling with free energy calculations. *Comp. Phys. Comm.* 135:40–57.